

ENHANCEMENT OF FAULT RIDE THROUGH CAPABILITY OF A WIND DRIVEN DFIG CONNECTED TO THE GRID

A. M. El-Sawy and Mahmoud A. Mossa

Electrical Engineering Department, Faculty of Engineering,

El-Minia University, EL-Minia, Egypt

E-mail: sawy1980@yahoo.com

(Received January 3, 2012 Accepted January 19, 2012)

Enhancement of fault ride-through (FRT) capability and subsequent improvement of rotor speed stability of wind farms equipped with doubly fed induction generator (DFIG) is the objective of this paper. The objective is achieved by employing a novel FRT scheme with suitable control strategy. The proposed FRT scheme, which is connected between the rotor circuit and dc link capacitor in parallel with Rotor Side Converter, consists of an uncontrolled rectifier, two sets of IGBT switches, a diode and an inductor. In this scheme, the input mechanical energy of the wind turbine during grid fault is stored and utilized at the moment of fault clearance, instead of being dissipated in the resistors of the crowbar circuit as in the existing FRT schemes. Consequently, torque balance between the electrical and mechanical quantities is achieved and hence the rotor speed deviation and electromagnetic torque fluctuations are reduced. This results in reduced reactive power requirement and rapid reestablishment of terminal voltage on fault clearance. Furthermore, the stored electromagnetic energy in the inductor is transferred into the dc link capacitor on fault clearance and hence the grid side converter is relieved from charging the dc link capacitor, which is very crucial at this moment. The converter in this case can be utilized to its full capacity for rapid restoration of terminal voltage and normal operation of DFIG. Extensive simulation study carried out employing MATLAB/SIMULINK software demonstrates the potential capabilities of the proposed scheme in enhancing the performance of wind farms DFIG to fault ride-through.

KEYWORDS: *DFIG, Fault ride-through (FRT), Low voltage ride-through (LVRT), Zero voltage ride-through (ZVRT), Rotor speed stability, power control of induction machines, PI controller.*

1. INTRODUCTION

The use of renewable energy sources for electric power generation is gaining importance in order to reduce global warming and environmental pollution, in addition to meeting the escalating power demand of the consumers. Among various renewable energy technologies, grid integration of wind energy electric conversion system is being installed in huge numbers due to their clean and economical energy conversion [1]. Recent advancements in wind turbine technology and power electronic systems are also more instrumental for the brisk option of grid integration of wind energy conversion system [2]. Doubly fed induction generator (DFIG) wind based turbines

offer more advantages such as operation over wide range of rotor speeds, four-quadrant active and reactive power control capabilities with improved efficiency compared to other wind turbine technologies [3]. With back to back pulse width modulated (PWM) converters connected in the rotor circuit of induction machine known as rotor side converter (RSC) and grid side converter (GSC), independent control of real power/speed and reactive power can be achieved by employing vector control method [4]. The main advantage of DFIG is that the converters carry only a fraction (25–30%) of the total power; hence the losses in the power electronic converters and their cost are considerably less [4].

LIST OF SYMBOLS

B	friction damping coefficient, N.m./rad./sec	R_s	stator winding resistance, Ω
I_{rdc}	rectified Rotor current, A	t_f	fault duration, sec
i_{ds}^e, i_{qs}^e	d^e -axis and q^e -axis stator currents	T_e	electromagnetic torque, N.m
i_{ds}^s, i_{qs}^s	d^s -axis and q^s -axis stator currents	T_m	mechanical torque in the shaft, N.m
i_{dr}^e, i_{qr}^e	d^e -axis and q^e -axis rotor currents	V_w	wind speed, m./sec
i_{dr}^s, i_{qr}^s	d^s -axis and q^s -axis rotor currents	V_{dr}^e, V_{qr}^e	d^e -axis and q^e -axis rotor voltages
i_{md}^e, i_{mq}^e	d^e -axis and q^e -axis magnetizing currents	V_{ds}^e, V_{qs}^e	d^e -axis and q^e -axis stator voltages
J_m	machine moment of inertia, Kg.m ²	V_{ds}^s, V_{qs}^s	d^s -axis and q^s -axis stator voltages
L	storage inductance, H	Symbols:	
L_m	magnetizing inductance, H	ω_r	electrical rotor angular speed in rad./sec
L_{ls}	stator leakage inductance, H	θ_e	electrical stator flux angle, degree
L_{lr}	rotor leakage inductance, H	θ_r	electrical rotor angular position, degree
L_r	rotor self inductance, H	θ_{slip}	electrical slip flux angle, degree
L_s	stator self inductance, H	σ	the leakage factor
p	d/dt, the differential operator	Subscripts:	
P	number of pole pairs	d-q	direct and quadrature axis
P_m	turbine power, W	s,r	stator and rotor, respectively
P_s, Q_s	stator active and reactive power	*	denote the reference value
R_{cw}	crowbar resistance, Ω	^	denote the estimated value
R_r	rotor winding resistance, Ω	+, -	denote the positive and negative components

In the past, the protection requirements of wind turbines were focused on safeguarding the turbines themselves. When the network suffers any transient disturbance such as voltage sag or short circuit fault, the wind turbine generators are usually disconnected from the grid as soon as the occurrence of voltage dip in the range of 70–80% [5]. However, with large integration of wind generators in the power system network, loss of considerable part of wind generators following a transient disturbance is not preferable. Tripping of numerous wind generators during transient disturbance can further risk the stability of power system thereby contributing to amplification of the effect of the disturbance that has originated. According to recent grid code requirement [5], wind generators should remain connected and actively support the grid during network fault or any other transient disturbance. Therefore, it has become inevitable for existing and new upcoming wind generators to be equipped with “fault ride-through (FRT) or low voltage ride-through (LVRT) or zero voltage ride through (ZVRT) schemes” to avoid their disconnection from the power system network during grid faults. Moreover, FRT is extremely important for maintaining system reliability and voltage stability, especially in areas where concentration of wind power generation facilities are high.

As a result of grid fault, the DFIG terminal voltage drops to a very low value, which is accompanied with increased stator current. The stator disturbance is further transmitted to the rotor because of magnetic coupling between the stator and rotor, thereby resulting in high transient rotor current. As the stator–rotor turns ratio of DFIG is chosen according to the desired variable speed range, it may not be possible to obtain the required rotor voltage from RSC to control high rotor current during grid faults. Current control techniques are usually adopted to limit the rotor current, which however leads to high voltage at the converter terminals that may harm the RSC.

The traditional method to protect the RSC of DFIG is to short circuit the rotor windings using a “thyristor crowbar” circuit [6]. Thyristor crowbar is usually made of anti-parallel thyristors or a diode bridge with anti-parallel thyristors and additional resistors if needed. The external resistors are employed to reduce the rotor current on fault occurrence and the reactive power requirement of the induction machine on fault clearance [7]. The thyristor crowbar is enabled and signals to RSC are blocked whenever the rotor current exceeds its limit. The crowbar and RSC recover to the pre-fault condition after the terminal voltage is restored above certain value following fault clearance. Hansen and Michalke have utilized power factory DIGSILENT, a power system simulation toolbox, to study the FRT capability of wind turbines [8]. A supplementary damping controller to damp the torsional oscillations in the wind turbine shaft that may affect the converter operation during grid faults was investigated. In addition, criteria for selection of size of crowbar resistance based on the parameters namely rotor current, electromagnetic torque and reactive power were demonstrated. The results of the analysis show that a small value of crowbar resistance causes high rotor current and torque transient peaks at the fault moment. A high value of crowbar resistance can however imply a risk of excessive transients in rotor current, electromagnetic torque and reactive power at the instant of removal of crowbar circuit. In [9], a soft transition from transient condition to normal operation with thyristor crowbar circuit is attempted by setting the reference values for the controllers equal to the values of currents at the moment of fault clearance. These values are then slowly

ramped up to the required reference values. In spite of the above, with thyristor crowbar scheme, transients could not be avoided at the resumption of normal operation.

Seman et al. have proposed an active crowbar circuit employing fully controllable bidirectional switches to protect the converters of DFIG [10]. The operation of active crow bar is controlled by dc link voltage. However, the dc link voltage alone is not a suitable candidate for the control of active crowbar circuit as it does not reflect the increase in rotor current under all situations. Using crowbar protection scheme, the input mechanical energy from the wind turbine is dissipated as heat in the crowbar circuit during the fault period. Hence, this method needs to confront the troublesome evacuation of heat generated in the resistors of the crowbar circuit during severe faults [11].

An additional anti-parallel thyristor switch in the stator circuit to limit the stator current subsequent to the instant of fault clearing was proposed in [12]. This method requires an additional switch with the rating of stator circuit and also it disconnects the stator winding during fault and completely interrupts stator active power generation. The impediment situation in all the above solution methods is troublesome evacuation of heat generated in the resistors of the crowbar circuit for a long-duration voltage sag or interruption. Moreover, the speed deviation that is resulted by a grid disturbance could not be averted in both thyristor and active crowbar FRT schemes. Hence with the above schemes, the reactive power requirement of DFIG at the instant of fault clearance is higher than the pre-fault value. Therefore, an attempt is made in this paper employing a simple additional circuitry instead of resistor crowbar circuit to temporarily store the input mechanical energy of the wind turbine during the fault period and subsequently utilize the same for charging of DC link capacitor on fault clearance.

In this paper, a novel FRT scheme is proposed. In this scheme, the input mechanical energy of the wind turbine during grid fault is stored and utilized at the moment of fault clearance, instead of being dissipated in the resistors of the crowbar circuit as in the existing FRT schemes. The proposed FRT scheme, which is connected between the rotor circuit and dc link capacitor in parallel with RSC, consists of an uncontrolled rectifier, two sets of IGBT switches, a diode and an inductor. As these components are rated for rotor circuit power ratings, the proposed scheme is cost effective.

The objective of the proposed scheme which employs minimal additional hardware components and simple control technique for successful fault ride-through of DFIG are:

- Satisfactory performance and compliance with grid code requirements.
- Protection of both generator converters against over-current and dc link capacitor against excessive over-voltage.
- Enhancing the stability of DFIG by damping speed deviations and electromagnetic torque fluctuations.
- Reduction of reactive power requirement of DFIG with rapid reestablishment of terminal voltage at fault clearance.

The rest of the paper is organized into following sections. Basic control structure and operation of DFIG is briefly presented in the next section. In Section 4,

the proposed FRT scheme with a suitable control technique for performance enhancement of DFIG is presented. An extensive analysis and performance evaluation of proposed FRT scheme under single line to ground fault condition at the generator terminals is carried out by simulation using MATLAB/SIMULINK software, which is presented in Section 5. The imperative results obtained with the proposed FRT scheme are included in the concluding remark.

2. MODEL OF THE DFIG SYSTEM UNDER UNBALANCED NETWORK

The unbalanced three-phase quantities such as voltage, current, and flux may be decomposed into positive and negative sequence components, assuming no zero sequence components. In the stationary (α - β) reference frame, the voltage, current, and flux can be decomposed into positive and negative sequence components as [13], [14].

$$F_{\alpha\beta}(t) = F_{\alpha\beta+}(t) + F_{\alpha\beta-}(t) = |F_{\alpha\beta+}|e^{-j(\omega_s t + \phi^+)} + |F_{\alpha\beta-}|e^{-j(\omega_s t + \phi^-)} \tag{1}$$

Where ϕ^+ and ϕ^- are the respective phase shift for positive and negative sequence components.

Figure 1 shows that, for the positive $(d-q)^+$ reference frame, the d^+ axis is fixed to the positive stator flux rotating at the speed of ω_s . While for the negative $(d-q)^-$ reference frames, as can be seen from figure 1, its d^- axis rotates at an angular speed of $-\omega_s$ with the phase angle to the α -axis being $-\theta_s$.

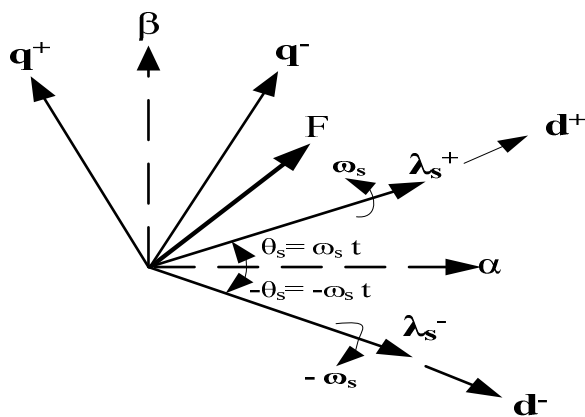


Figure.1. Relationships between the (α - β) reference frame and the $(d-q)^+$ and $(d-q)^-$ reference frames.

From figure.1, the transformation from (α - β) reference frame to $(d-q)^+$ and $(d-q)^-$ reference frames are given by,

$$F_{dq}^+ = F_{\alpha\beta} \cdot e^{j\omega_s t} = F_{dq}^- \cdot e^{+j2\omega_s t} \tag{2}$$

$$F_{dq}^- = F_{\alpha\beta} \cdot e^{-j\omega_s t} = F_{dq}^+ \cdot e^{-j2\omega_s t} \quad (3)$$

Similar to grid connected converters [14], during network unbalance, the state space form of the rotor model can be expressed in the positive and negative sequence components, rotating at angular frequency of ω_s and $-\omega_s$, respectively a:

$$p \begin{bmatrix} I_{dr}^+ \\ I_{qr}^+ \end{bmatrix} = \begin{bmatrix} -\frac{R_r}{\sigma L_r} & (\omega_s - \omega_r) \\ -(\omega_s - \omega_r) & -\frac{R_r}{\sigma L_r} \end{bmatrix} \begin{bmatrix} I_{dr}^+ \\ I_{qr}^+ \end{bmatrix} + \frac{L_m(\omega_s - \omega_r)}{\sigma L_r L_s} \begin{bmatrix} \lambda_{qs}^+ \\ -\lambda_{ds}^+ \end{bmatrix} + \frac{1}{\sigma L_r} \begin{bmatrix} V_{dr}^+ \\ V_{qr}^+ \end{bmatrix} \quad (4)$$

$$p \begin{bmatrix} I_{dr}^- \\ I_{qr}^- \end{bmatrix} = \begin{bmatrix} -\frac{R_r}{\sigma L_r} & (-\omega_s - \omega_r) \\ -(-\omega_s - \omega_r) & -\frac{R_r}{\sigma L_r} \end{bmatrix} \begin{bmatrix} I_{dr}^- \\ I_{qr}^- \end{bmatrix} + \frac{L_m(-\omega_s - \omega_r)}{\sigma L_r L_s} \begin{bmatrix} \lambda_{qs}^- \\ -\lambda_{ds}^- \end{bmatrix} + \frac{1}{\sigma L_r} \begin{bmatrix} V_{dr}^- \\ V_{qr}^- \end{bmatrix} \quad (5)$$

According to figure.1 and equations (1), (2), and (3), the stator and rotor current and voltage vectors can be expressed using their respective positive and negative sequence components as:

$$V_{dqs} = V_{dqs}^+ + V_{dqs}^- \cdot e^{-j2\omega_s t} \quad (6)$$

$$V_{dqr} = V_{dqr}^+ + V_{dqr}^- \cdot e^{-j2\omega_s t} \quad (7)$$

Although unbalanced, the stator voltage can still be regarded as being constant. Therefore,

$$p\lambda_{dqs}^+ = 0.0, \quad p\lambda_{dqs}^- = 0.0 \quad (8)$$

Under unbalanced network conditions, the amplitude and rotating speed of the stator flux are no longer constant. Neglecting the stator resistance and taking into account equations (6), (7) and (8), the stator voltage and current can be expressed in the positive $(d-q)^+$ reference frame as:

$$\vec{V}_{dqs} = j\omega_s (\lambda_{dqs}^+ - \lambda_{dqs}^- \cdot e^{-j2\omega_s t}) \quad (9)$$

$$\vec{I}_{dqs} = \frac{1}{L_s} (\lambda_{dqs}^+ + \lambda_{dqs}^- \cdot e^{-j2\omega_s t}) - \frac{L_m}{L_s} (I_{dqr}^+ + I_{dqr}^- \cdot e^{-j2\omega_s t}) \quad (10)$$

Similar to balanced condition, the stator output active and reactive powers can be calculated as:

$$P_s + jQ_s = -\frac{3}{2} \vec{V}_{dqs} \times \vec{I}_{dqs} \quad (11)$$

Where \times is the cross product of two vectors \vec{V}_{dqs} and \vec{I}_{dqs} .

Substituting (9) and (10) into (11) and separating the active and reactive power into different oscillating components yield,

$$\begin{aligned} P_s &= P_{s0} + P_{s\sin 2} \cdot \sin(2\omega_s t) + P_{s\cos 2} \cdot \cos(2\omega_s t) \\ Q_s &= Q_{s0} + Q_{s\sin 2} \cdot \sin(2\omega_s t) + Q_{s\cos 2} \cdot \cos(2\omega_s t) \end{aligned} \quad (12)$$

Where

$$\begin{aligned}
 P_{s0} &= \frac{3L_m \omega_s}{2L_s} [-\lambda_{qs}^+ I_{dr}^+ + \lambda_{ds}^+ I_{qr}^+ + \lambda_{qs}^- I_{dr}^- - \lambda_{ds}^- I_{qr}^-] \\
 Q_{s0} &= \frac{3\omega_s}{2L_s} [-\lambda_{ds}^{+2} - \lambda_{qs}^{+2} + \lambda_{ds}^{-2} + \lambda_{qs}^{-2}] + \frac{3L_m \omega_s}{2L_s} [\lambda_{ds}^+ I_{dr}^+ + \lambda_{qs}^+ I_{qr}^+ - \lambda_{ds}^- I_{dr}^- - \lambda_{qs}^- I_{qr}^-] \\
 P_{sSin2} &= \frac{3\omega_s}{2L_s} [\lambda_{ds}^- \lambda_{ds}^+ + \lambda_{qs}^- \lambda_{qs}^+ + \lambda_{ds}^+ \lambda_{ds}^- + \lambda_{qs}^+ \lambda_{qs}^-] + \frac{3L_m \omega_s}{2L_s} [-\lambda_{ds}^- I_{dr}^+ - \lambda_{qs}^+ I_{qr}^+ - \lambda_{ds}^+ I_{dr}^- - \lambda_{qs}^- I_{qr}^-] \\
 P_{sCos2} &= \frac{3\omega_s}{2L_s} [-\lambda_{qs}^- \lambda_{ds}^+ + \lambda_{ds}^- \lambda_{qs}^+ + \lambda_{qs}^+ \lambda_{ds}^- - \lambda_{ds}^+ \lambda_{qs}^-] + \frac{3L_m \omega_s}{2L_s} [\lambda_{qs}^- I_{dr}^+ - \lambda_{ds}^- I_{qr}^+ - \lambda_{qs}^+ I_{dr}^- + \lambda_{ds}^+ I_{qr}^-] \\
 Q_{sSin2} &= \frac{3L_m \omega_s}{2L_s} [\lambda_{qs}^- I_{dr}^+ - \lambda_{ds}^- I_{qr}^+ + \lambda_{qs}^+ I_{dr}^- - \lambda_{ds}^+ I_{qr}^-] \\
 Q_{sCos2} &= \frac{3L_m \omega_s}{2L_s} [-\lambda_{ds}^- I_{dr}^+ - \lambda_{qs}^- I_{qr}^+ + \lambda_{ds}^+ I_{dr}^- + \lambda_{qs}^+ I_{qr}^-] \tag{13}
 \end{aligned}$$

According to figure.2, the electromagnetic power equals to the sum of the power outputs from the equivalent voltage source $j\omega_s \lambda_s$ and $j(\omega_s - \omega_r) \lambda_r$. Thus, it is given by,

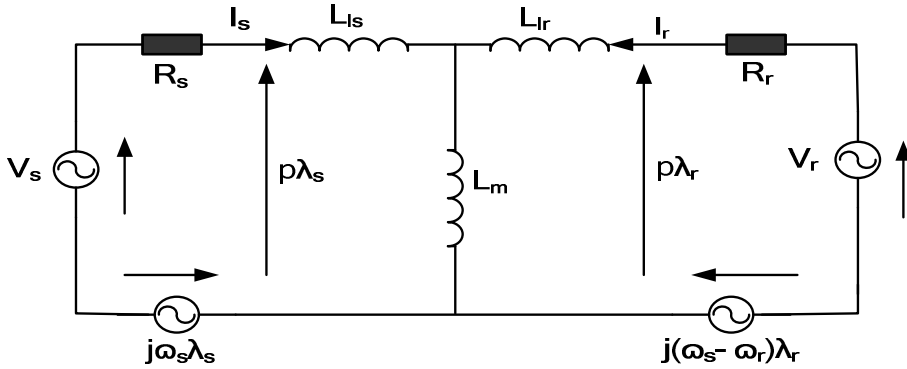


Figure 2. Equivalent circuit of a DFIG in the synchronous reference frame rotating at speed of ω_s .

$$\begin{aligned}
 P_e &= -\frac{3}{2} \text{Re}[j\omega_s \bar{\lambda}_{dqs}^+ \times \bar{I}_{dqs}^+ + j(\omega_s - \omega_r) \bar{\lambda}_{dqr}^+ \times \bar{I}_{dqr}^+] \\
 &= -\frac{3}{2} \text{Re}[j\omega_s \bar{\lambda}_{dqs}^+ \times \frac{1}{L_s} (\bar{\lambda}_{dqs}^+ - L_m \bar{I}_{dqr}^+)] - \frac{3}{2} \text{Re}[j(\omega_s - \omega_r) (\frac{L_m}{L_s} \bar{\lambda}_{dqs}^+ + \sigma L_r \bar{I}_{dqr}^+) \times \bar{I}_{dqr}^+] \\
 &= \frac{3}{2} \frac{L_m}{L_s} \omega_r \text{Re}[j \bar{\lambda}_{dqs}^+ \times \bar{I}_{dqr}^+] = P_{e0} + P_{eSin2} + P_{eCos2} \tag{14}
 \end{aligned}$$

Where,

$$\begin{bmatrix} P_{e0} \\ P_{e\sin 2} \\ P_{e\cos 2} \end{bmatrix} = \begin{bmatrix} -\lambda_{qs}^+ & \lambda_{ds}^+ & -\lambda_{qs}^- & \lambda_{ds}^- \\ \lambda_{ds}^- & \lambda_{qs}^- & -\lambda_{ds}^+ & -\lambda_{qs}^+ \\ -\lambda_{qs}^- & -\lambda_{ds}^- & -\lambda_{qs}^+ & \lambda_{ds}^+ \end{bmatrix} \begin{bmatrix} I_{dr}^+ \\ I_{qr}^+ \\ I_{dr}^- \\ I_{qr}^- \end{bmatrix} \quad (15)$$

The electromagnetic torque of the DFIG is calculated as:

$$T_e = \frac{P_e}{\omega_r} = (P_{e0} + P_{e\sin 2} + P_{e\cos 2}) / \omega_r \quad (16)$$

3. SYSTEM DESCRIPTION

Figure 3 shows a basic layout of a DFIG driven by a wind turbine system, the machine may be simulated as an induction machine having 3-phase supply in the stator and three phase supply in the rotor. The rotor circuit is connected through slip rings to the back to back converters arrangement controlled by pulse width modulation (PWM) strategies [15] and [16]. The rating of these converters is restricted for speed range of operation to a fraction of the machine rated power.

The voltage magnitude and power direction between the rotor and the supply may be varied by controlling the switch impulses that drive the IGBTs inverter. Back to back converters consist of two voltage source converters (ac-dc-ac) having a dc link capacitor connecting them. The generator side converter takes the variable frequency voltage and converts it into a dc voltage. The grid side (line side) converter has the voltage conversion from the dc link as input and ac voltage at grid as output. Rotor-side converter acts as a voltage source converter, while the grid-side converter is expected to keep the capacitor voltage constant under wind speed variations and at different operating conditions of the grid [17] and [18]. The current and voltage controllers of Figure 3 are included for obtaining the rotor side and line side voltage references (V_{abcr}^* and V_{abcl}^*).

4. CONTROL STRATEGY OF PROPOSED FRT SCHEME

Figure 4 shows the proposed block diagram of the DFIG driven by a wind turbine control system and FRT methodology. The control system consists of a reactive power controller, a torque controller, three current controllers, two co-ordinate transformations (C.T), two sinusoidal pulse-width-modulation (SPWM) for transistor bridge converters/inverters, a stator flux and torque estimators and reactive power calculator. The FRT scheme components are as shown, an uncontrolled rectifier, two sets of IGBT switches S1, S2, diode D and storage inductor L. The reference value of reactive power, Q_s^* , can be directly implemented to the converter, considering the appropriate power.

Individual control of the rotor side converter (RSC), of the line/grid side converter (GSC) and related feedback between the two converters are shown. A sinusoidal pulse width modulator (SPWM) provides field oriented currents i_{dr}^e and i_{qr}^e to the rotor circuit, controlling stator reactive power and electromagnetic torque,

respectively. The co-ordinate transformation (C.T)⁻¹ in Figure 4 is used for transforming these components to the three phase rotor voltage references by using the field angle.

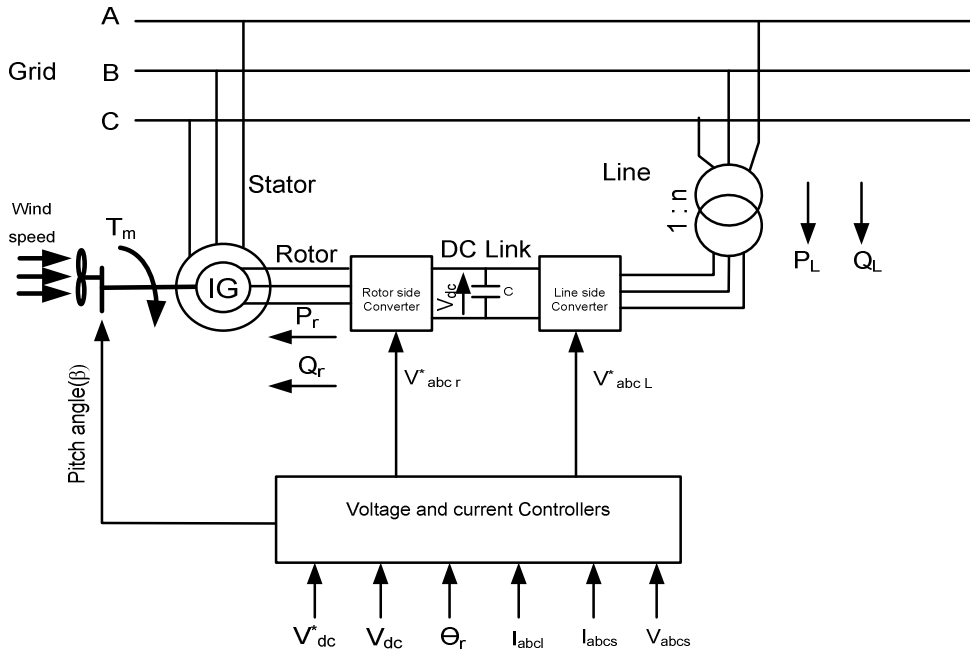


Figure 3: Doubly-fed induction Generator driven by a wind turbine System

The control inputs to the (SPWM) are the line voltage or rotor voltage commands and predefined triangular carrier waves. The SPWM modulator calculates the pulse pattern and supplies firing signals to the inverter. In the PWM scheme, the inverter output voltage is defined by the intersections of the voltage commands and carrier waves [20], which are synchronized such that the carrier frequency is multiple of the frequency of voltage commands. This manner of synchronization eliminates sub harmonic generation [19]. The reference Torque is given by the turbine optimal torque-speed profile. Another (SPWM) is used to interface with the power network, possibly through a transformer. In the same $d^e - q^e$ reference frame as determined by the stator flux, its currents (i_{qt}^e and i_{dt}^e) are also field oriented, controlling P_L and Q_L , respectively. As discussed earlier, P_L is controlled through i_{qt}^e to stabilize the dc bus voltage and Q_L is controlled through i_{dt}^e to meet the overall reactive power command.

The RSC controls the reactive power (Q) injection and the developed electric power (P_{elec}) given by the DFIG. The electric power reference (P_{opt}^*) is determined based on the optimum rotor speed depending on the wind speed as a parameter [21]. The calculated reactive power of the DFIG (Q^*) is compared to the estimated one. The reference direct axis current (I_{dr}^{e*}) is then calculated from the resulting (Q) error, through a PI controller. (I_{dr}^{e*}) is then compared to the actual direct axis rotor current

(i_{dr}^e), and the error is then sent to another PI controller to determine the reference value of the direct axis rotor voltage (V_{dr}^{e*}).

The quadrature axis component of the rotor current (I_{qr}^{e*}) is calculated in a similar manner as in the direct axis component, and is used to regulate the developed electric power (P_{elec}) to an optimal reference (P_{opt}^*). The direct-quadrature components of the reference rotor voltages (V_{dr}^{e*} and V_{qr}^{e*}) are then transformed back into the three-phase voltages (V_{abcr}^*), required at the RSC output, through a dq0-abc transformation. The converters IGBT's are considered to be ideal and commutation losses are therefore neglected.

The GSC controls the voltage level at the direct-current link (DC link) between the two converters. The DC link reference voltage level (V_{dc}^*) is set to 1200 V, this voltage is compared to the actual voltage and from the resulting error the direct axis component of the reference line current (I_{dl}^{e*}) is being calculated through a PI controller. (I_{dl}^{e*}) is then compared to the actual value of the direct axis line current (I_{dl}) and then sent to another PI controller, in order to calculate the direct axis reference line voltage (V_{dL}^{e*}).

There is no need for a GSC reactive power regulation, since the RSC already controls the power factor of the DFIG. Therefore the quadrature axis component of the reference current is set to zero ($I_{ql}^{e*} = 0$). I_{ql}^{e*} is then compared to the quadrature axis component of the actual line current (I_{ql}) and the error is sent to a PI controller to determine the quadrature axis component of the reference line voltage (V_{qL}^{e*}). The two components of the reference line voltage (V_{dL}^{e*} and V_{qL}^{e*}) are then transformed into the three-phase voltages (V_{abcl}^*) needed at the output of the GSC.

The method uses the stator reference frame model of the induction machine and the same reference frame is used in the implementation thereby avoiding the trigonometric operations encountered in the C.T of other reference frames. This is one of the advantages of the control scheme.

During normal operation, the IGBT switches S1 and S2 remain open and diode D is reverse biased, therefore the proposed FRT scheme does not interfere the normal operation of DFIG.

During grid faults, DFIG terminal voltage drops to a very low value and the stator current rises rapidly. The stator disturbance is further transmitted to the rotor because of magnetic coupling between them. This will result in high transient current in the rotor circuit that may damage the power electronic devices in the rotor converter. In order to protect the converter, gating signals to RSC are blocked whenever the rotor current exceeds the semiconductor device ratings. This increase was avoided by using a de-saturation detection technique [22], provides the state of electrical over stress of IGBT under current fault condition when gate voltage is high. Reducing gate voltage in a controlled manner to just above gate threshold voltage is preferred. This will reduce fault current and after some finite time gate voltage is brought down to zero safely, turning off the IGBT without stress. Though the devices are now protected, the transient current in the rotor circuit now raises the dc link voltage through the anti-parallel diodes of RSC. Therefore, a suitable control technique is proposed in this paper so as to protect the rotor converter against over-current and the dc link capacitor against excessive over-voltage.

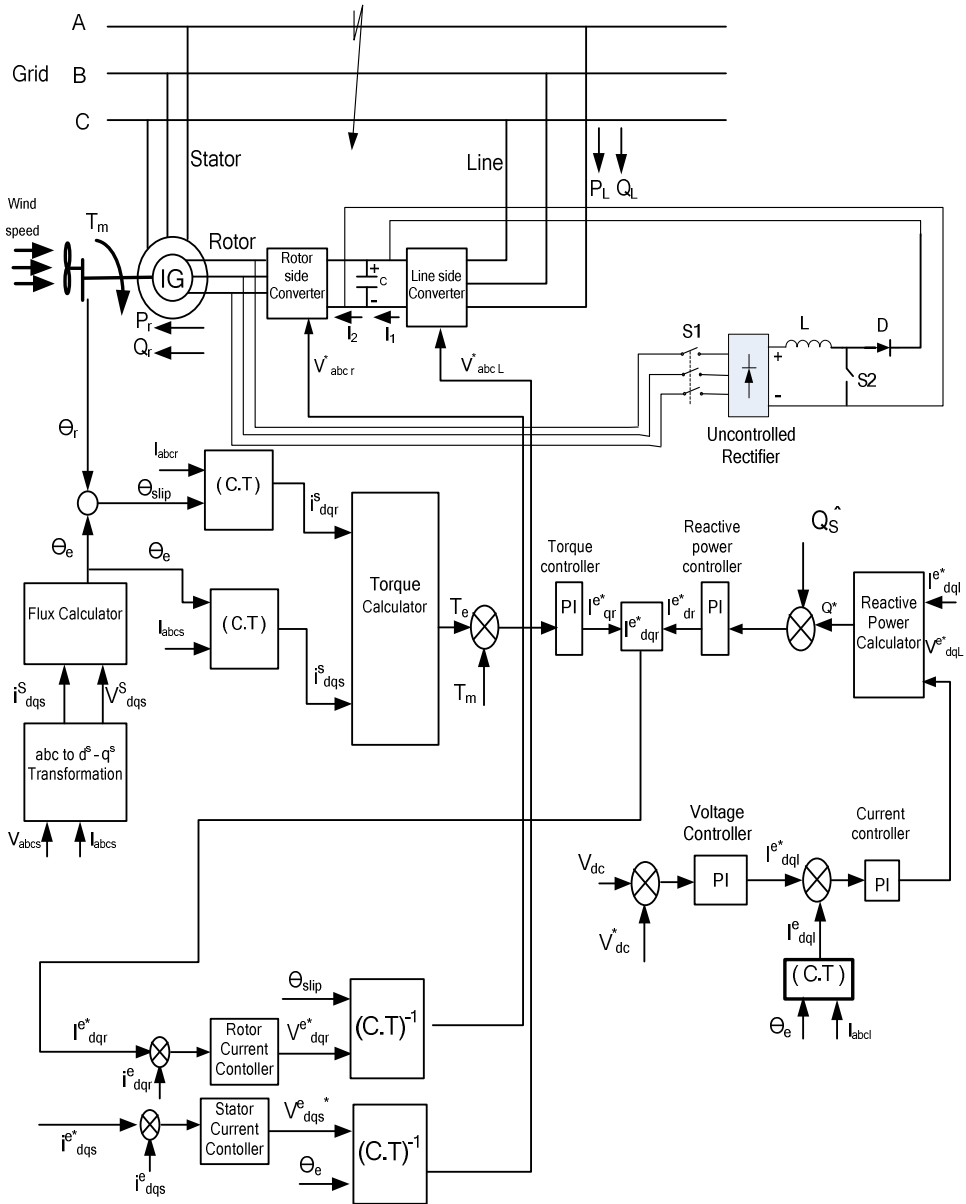


Figure 4. Proposed fault ride-through scheme and control for a wind driven DFIG system.

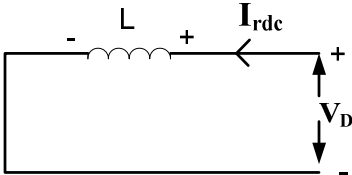
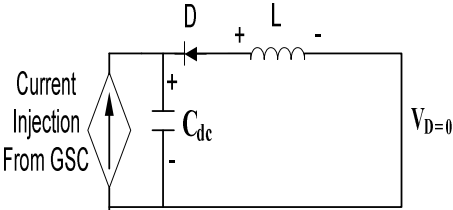
4.1. Sequence and mode of operation of proposed FRT scheme

The mode and sequence of operation of the proposed FRT scheme is shown in Table 1. In the proposed FRT scheme, when the rotor current is more than the permissible limit, gating signals to RSC are blocked. Simultaneously, the switches S1 and S2 are closed if either the terminal voltage dip is more than the threshold value or the dc link capacitor voltage goes beyond the permissible limit. Since the generator and converter

stay connected, the synchronism of operation remains established during and after the fault. Normal operation can be restored immediately after the fault is cleared. As soon as the rotor current decreases below the permissible limit, gating signals to RSC are restored unlike the crowbar protection scheme, where the gating signals to RSC are established only after the terminal voltage restores above a certain limit [23]. Thus, generator magnetization is done over the rotor circuit with the help of RSC. Now the input mechanical energy of the wind turbine is stored as electromagnetic energy in the inductor L. Since a torque balance is established between the developed electromagnetic torque of induction machine and the input mechanical torque of the wind turbine, the rotor speed deviation is reduced. Thus the reactive power requirement of DFIG on fault clearance is also reduced in accordance with the reduction in the rotor speed deviation [23] with the help of proposed FRT scheme.

On fault clearing, when the voltage dip is reduced below the threshold value, the switches S1 and S2 are opened. Now the diode D gets forward biased and the stored energy in the inductor L is transferred into the dc link capacitor C_{dc}. Consequently, the GSC current needed for charging the dc link capacitor is reduced and the converters can be used to its full capacity in restoring the normal operation of DFIG.

Table 1. Sequence and mode of operation of proposed FRT scheme.

On fault occurrence (Mode-1)	On fault clearance (Mode-2)
<ul style="list-style-type: none"> • If the rotor current exceeds the permissible limit, block gating signals to the RSC. • Measure the terminal voltage and compute the voltage dip (ΔV). • If either the voltage dip (ΔV) is more than the threshold value or dc link voltage level exceeds its limit, connect the proposed FRT scheme by closing the switches S1 and S2. • After initial rotor current transients die out, restore gating signals to RSC when the rotor current reduces below the permissible limit. <p>Input mechanical energy of the wind turbine is stored in inductor L of the proposed FRT scheme through uncontrolled rectifier and switches S1 and S2.</p>  <p>IGBT Switches S1 and S2 are closed</p>	<ul style="list-style-type: none"> • Measure the terminal voltage and compute the voltage dip (ΔV). • If the voltage dip (ΔV) is less than the threshold value, disconnect the FRT scheme by opening the switches S1 and S2. • The stored electromagnetic energy in the inductor is transferred into the dc link capacitor.  <p>IGBT Switches S1 and S2 are opened</p>

4.2. Choice of size of storage inductor

The selection of the size of inductor L in the proposed FRT scheme is similar to that of the crowbar resistance scheme. Small value of crowbar resistance (R_{cw}) does not limit the rotor current and cause torque transient peaks during the fault moment. Higher R_{cw} has an efficient damping effect on the rotor current and electromagnetic torque. It also reduces the reactive power requirement at the instant of fault clearing. However, a very high value of R_{cw} can imply a risk of excessive transients in rotor current, torque and reactive power while removing the crowbar [24]. Similarly, if the inductor size is too small, the entire mechanical energy of the wind turbine during the transient period cannot be stored. Large inductor size will make the scheme bulky and costly. Considering the correct choice of R_{cw} obtained for an existing DFIG machine, a procedure is presented in this section to acquire an initial guess for the choice of storage inductor L .

In the proposed FRT scheme, in order to achieve a performance equivalent to that of the active crowbar scheme, the energy content of the storage inductor should be at least equal to the energy dissipation capacity of the crowbar resistor R_{cw} in active crowbar scheme. With this hypothesis, the size of storage inductor is computed as follows.

Neglecting switching losses in the power electronic devices, the energy dissipated in the resistor R_{cw} of an active crowbar FRT scheme during the fault event is given by

$$E_{cw} = I_{rdc}^2 R_{cw} t_f \tag{17}$$

Where I_{rdc} is the Rectified Rotor current (A); R_{cw} , the Crowbar resistance (Ω) and t_f is the Fault duration (s).

During same fault duration, assuming that I_{rdc} is constant during fault period, the energy required to be stored in inductor L , employing the proposed FRT scheme is given by

$$E_L = \frac{1}{2} I_{rdc}^2 L \tag{18}$$

Where L is the storage inductance in (H).

Based on the hypothesis, that the capacity of energy content of the inductor should be greater than or at least equal to the dissipation capacity of the resistors R_{cw} in the crowbar FRT scheme, i.e.

$$E_L \geq E_{cw} \tag{19}$$

Thus, from equations (17) and (19),

$$\frac{1}{2} I_{rdc}^2 L \geq I_{rdc}^2 R_{cw} t_f \tag{20}$$

From (20), the choice of inductor size is computed as,

$$L \geq 2R_{cw} t_f \tag{21}$$

Equation (21) is a good starting point for selection of the inductor size in the proposed FRT scheme.

The crowbar resistance (R_{cw}) is chosen as 1.486Ω ($R_{cw} = 20R_r$), where R_r is the rotor resistance as recommended in [24] and utilized in [25]. As wind generators are expected to be disconnected from the grid for fault duration longer than $t_f = 0.5s$ [7, 8], the size of the inductor utilized in the proposed scheme is computed as follows:

$$(R_{cw} = 20R_r); t_f = 0.5s; \text{ Using (21), } L \geq 2R_{cw}t_f; L \geq 0.38H$$

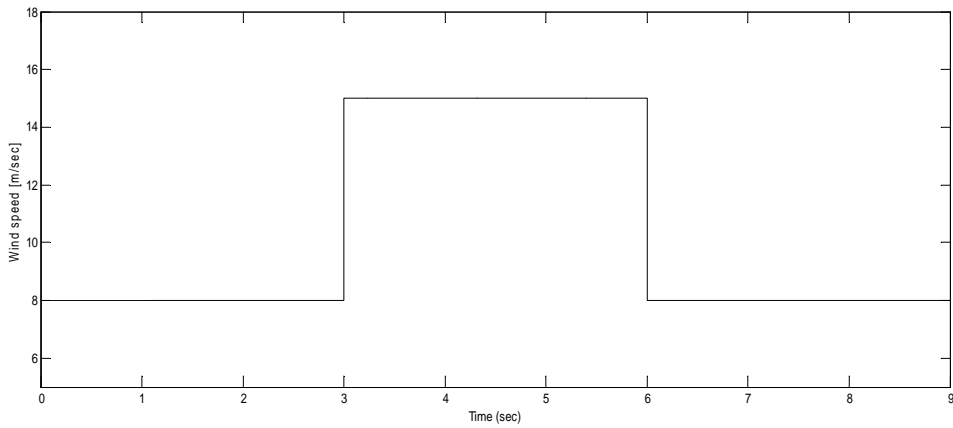
Therefore, an inductor of $L = 0.5 H$ is chosen for the simulation study.

5. SIMULATION RESULTS AND DISCUSSIONS

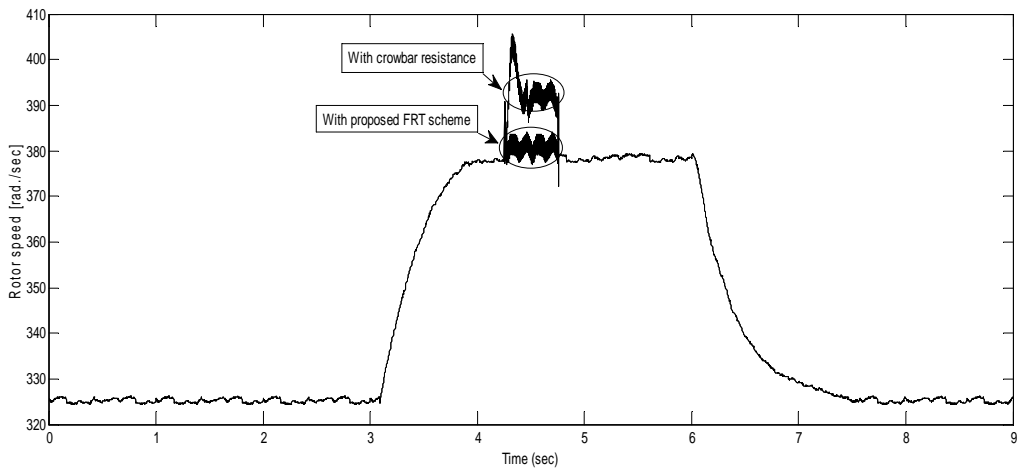
Digital simulation is carried out in order to validate the effectiveness of the proposed scheme of Figure 4. The Matlab/Simulink software package has been used for this purpose. The DFIG under study is a 9 MW, 6-poles, 967 rpm and its nominal parameters and specifications are listed in table [2]. Two types of faults, symmetrical (three phase to ground fault) and unsymmetrical (single line to ground fault) were applied across the grid terminals and the results are as follows:

Table [2]. Nominal Parameters of DFIG and Wind turbine.

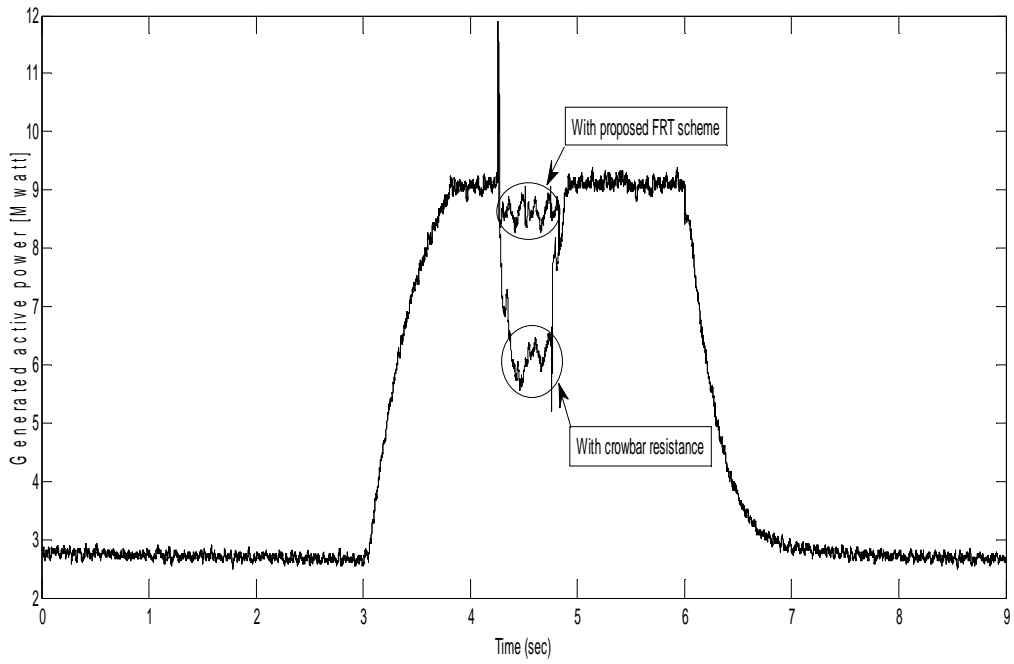
DFIG and Wind turbine parameters	
$P_n(\text{nominal})$	$9 \times 10^6 \text{ W}$
$V_n(\text{rms})$	580 V
F_n	50 Hz
R_s	0.104Ω
R_r	0.0743Ω
L_{ls}	2.54 (H)
L_{lr}	2.31 (H)
L_m	4.35 (H)
$V_{dc}(\text{nominal})$	1200 V
J_m	0.0887 Kg.m^2
B	$0.00478 \text{ N.m./rad./s.}$
DC bus capacitor	$6 \times 10000 \mu\text{F}$
Nominal mechanical output power of turbine, at $V_w = 12 \text{ m/s.}$ $\rho = 1.25 \text{ Kg./m}^2.$	$9 \times 10^6 \text{ W}$



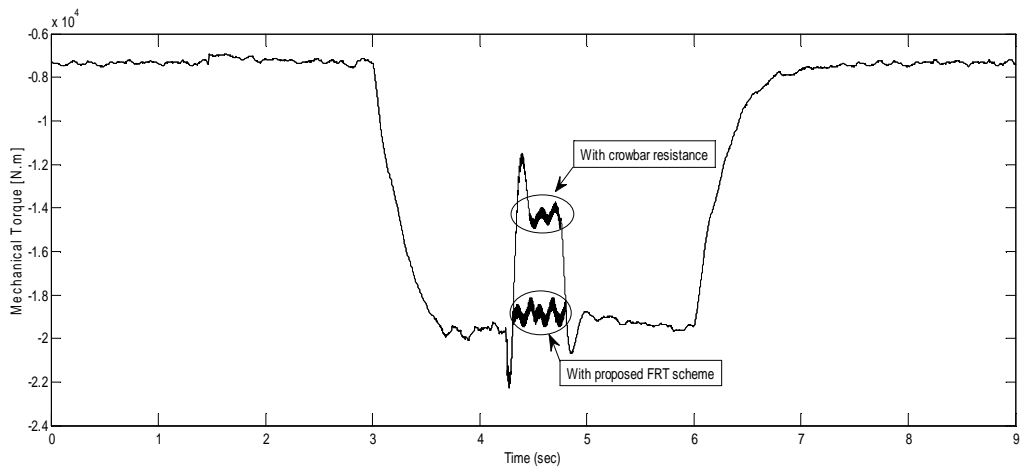
(a) Wind speed variation (m/sec)



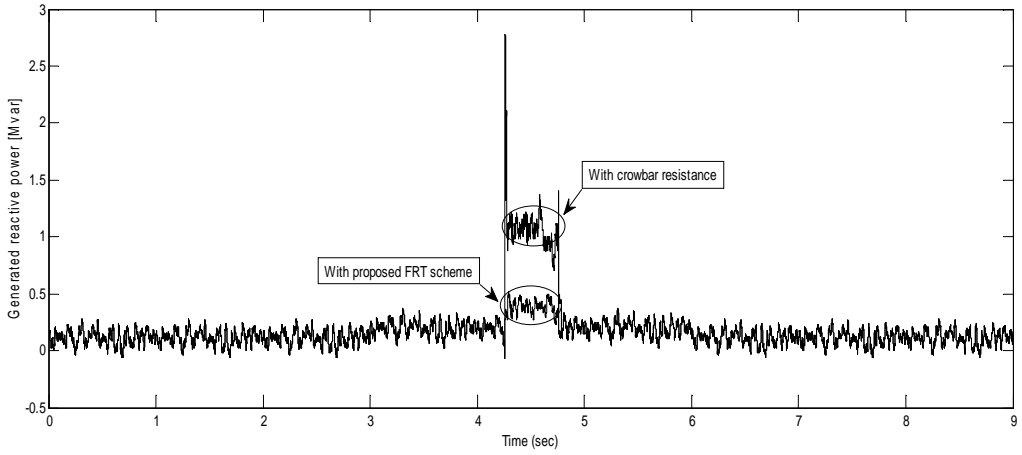
(b) Rotor speed (rad./sec)



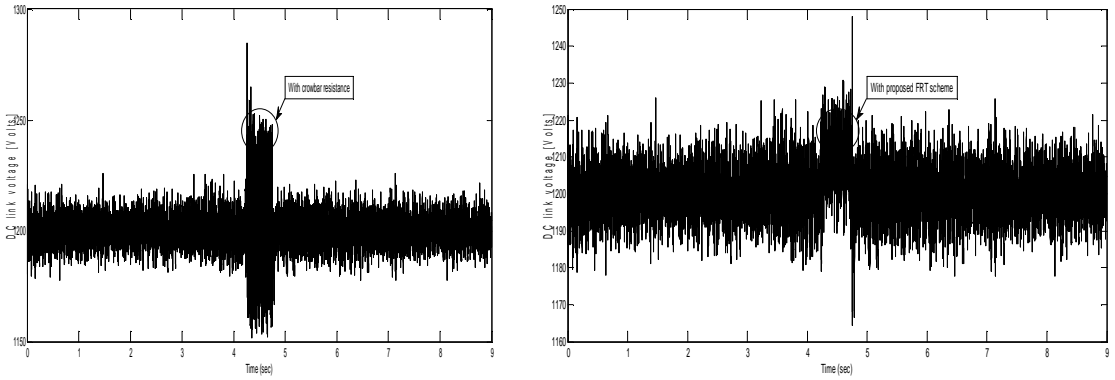
(c) Generated active power (Mwatt)



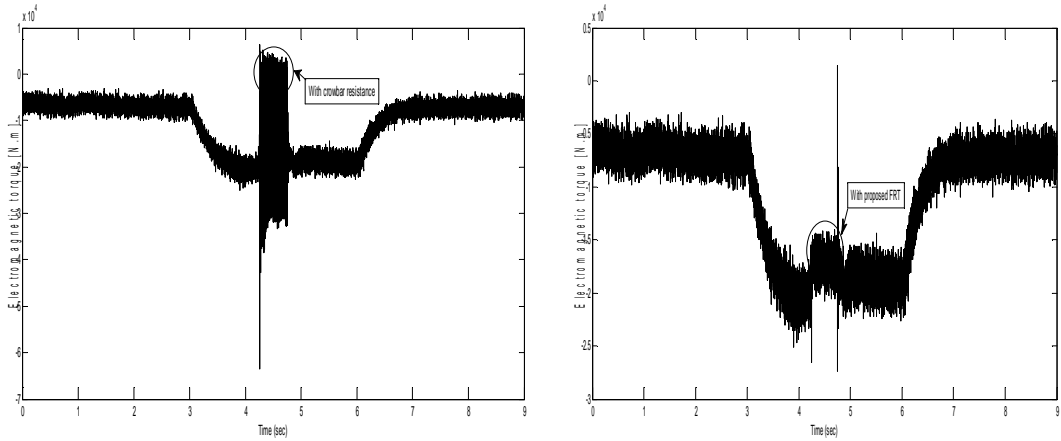
(d) Mechanical torque (N.m)



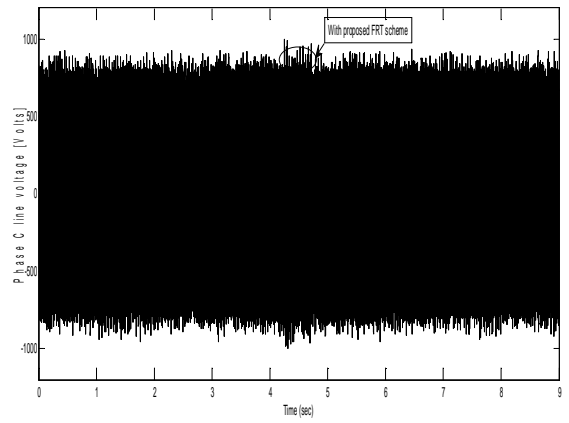
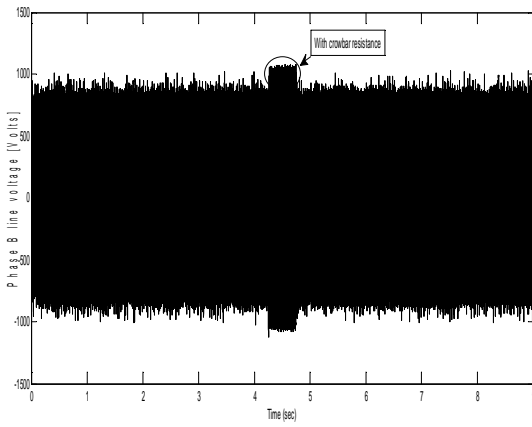
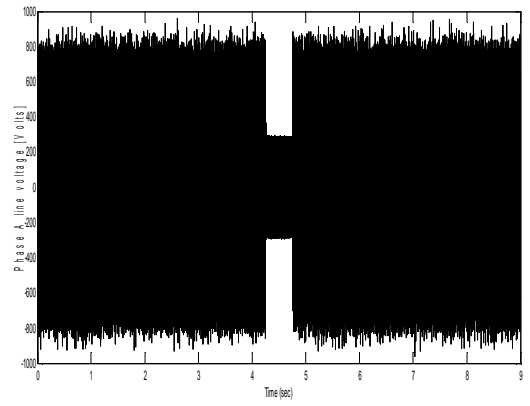
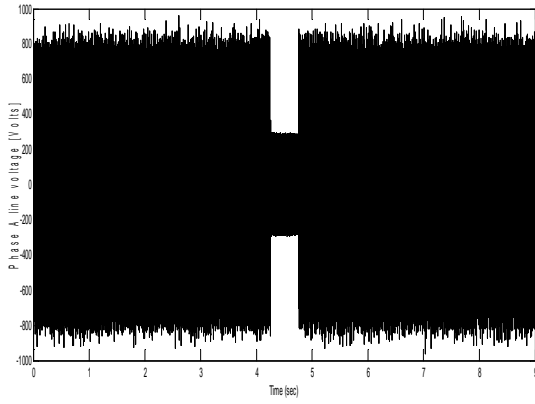
(e) Generated reactive power (Mvar)

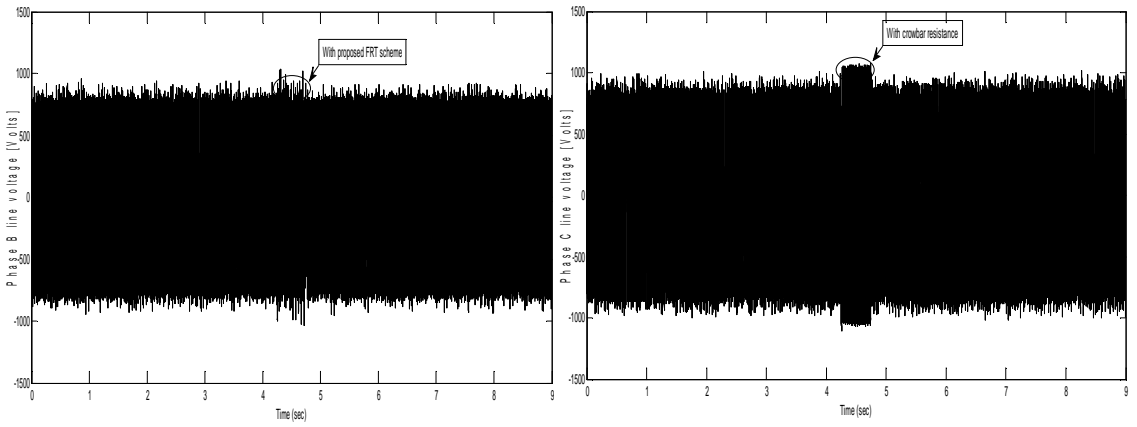


(f) DC link Voltage with and without applying FRT scheme (Volts)

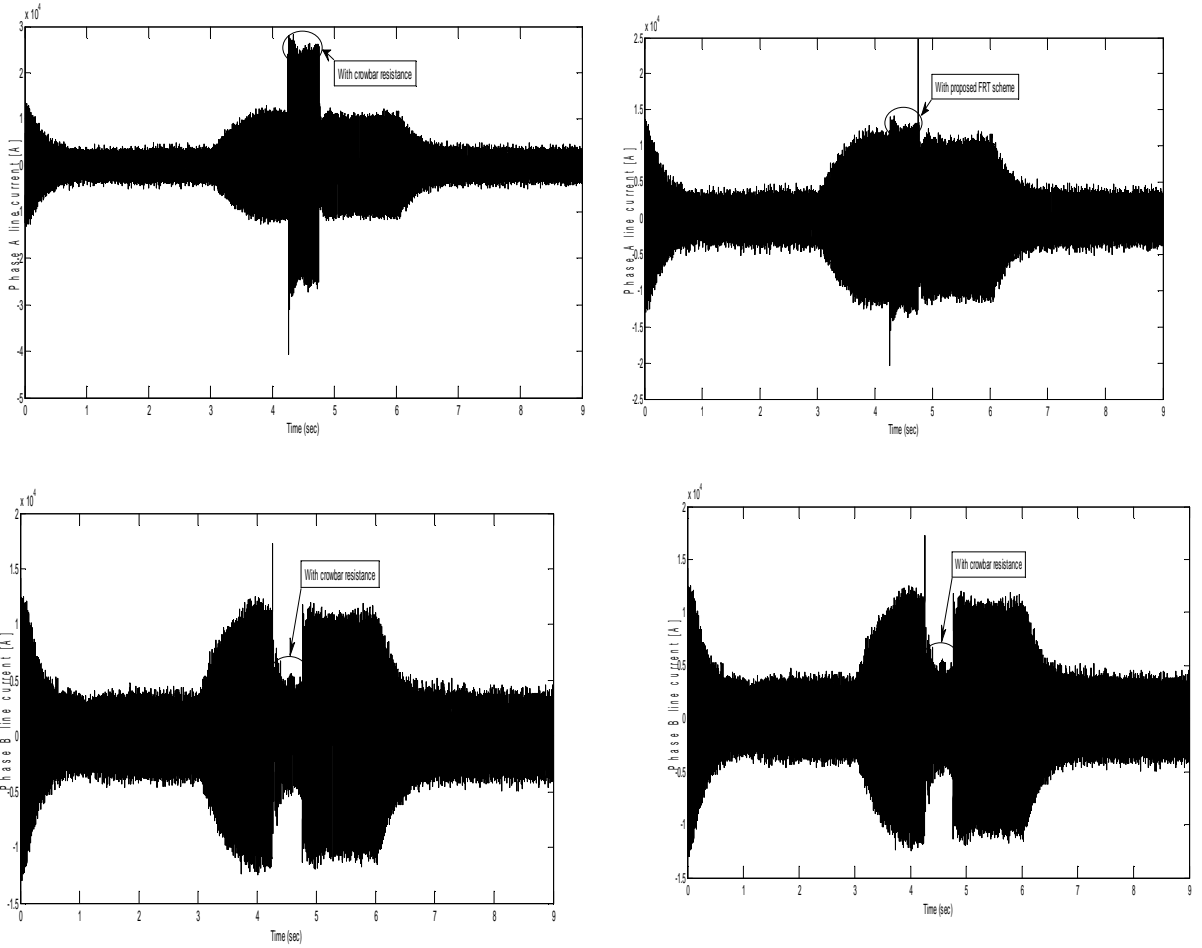


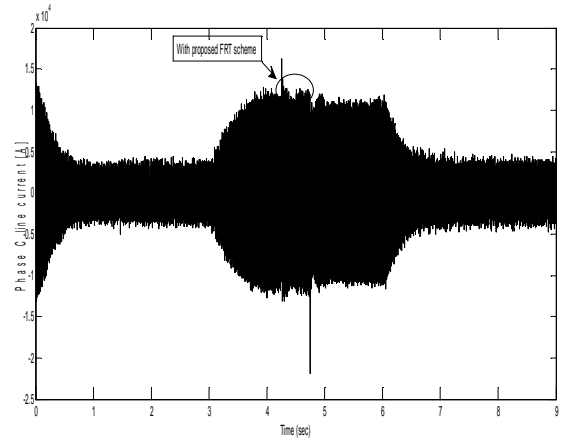
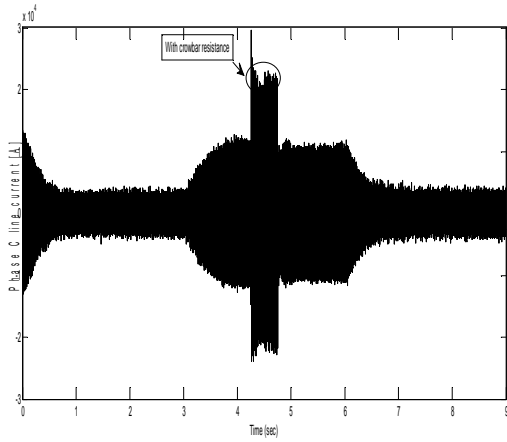
(g) Electromagnetic torque with and without applying FRT scheme (N.m)



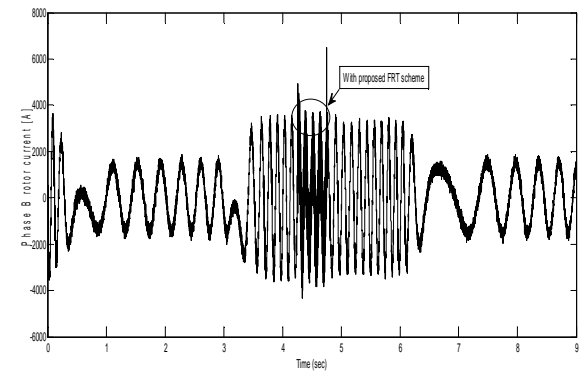
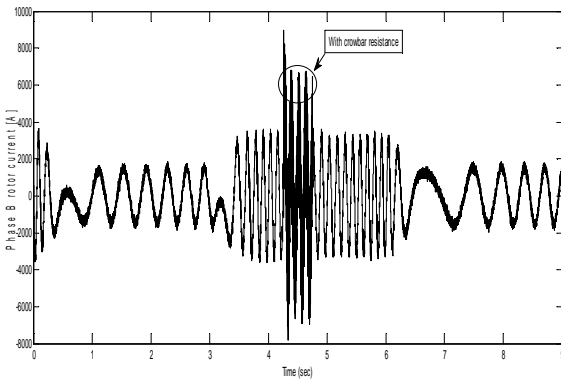
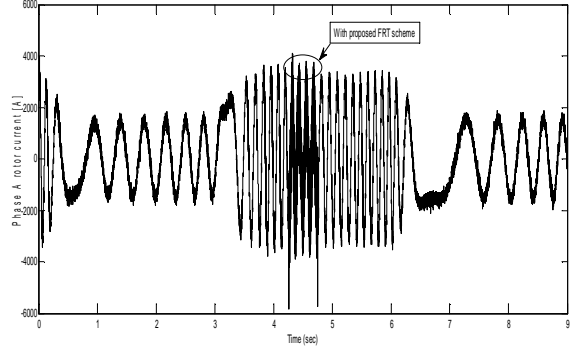
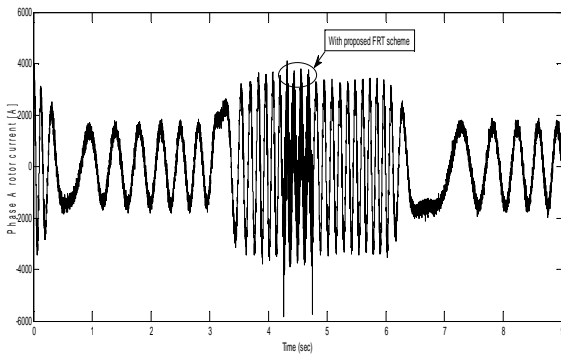


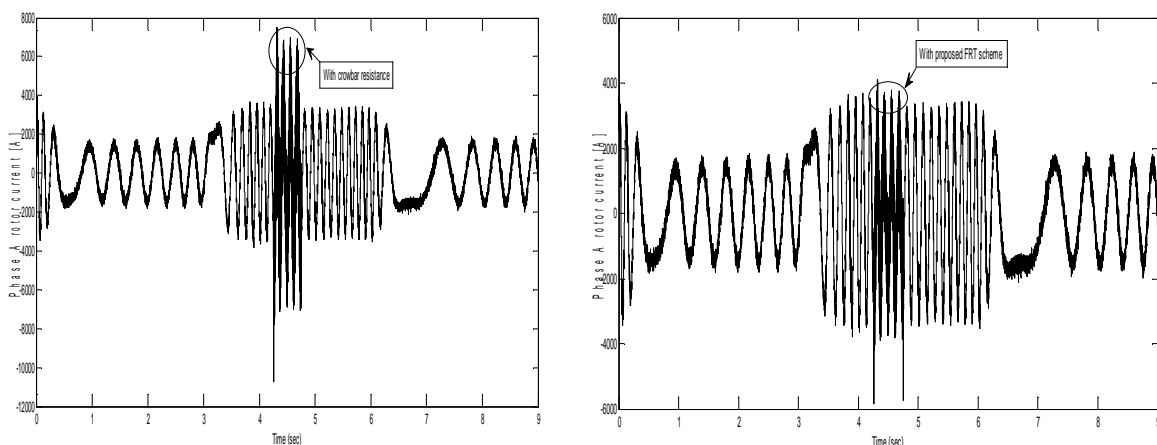
(h) Line voltages with and without applying FRT scheme (Volts)





(i) Line currents with and without applying FRT scheme (A)





(j) Rotor currents with and without applying FRT scheme (A)

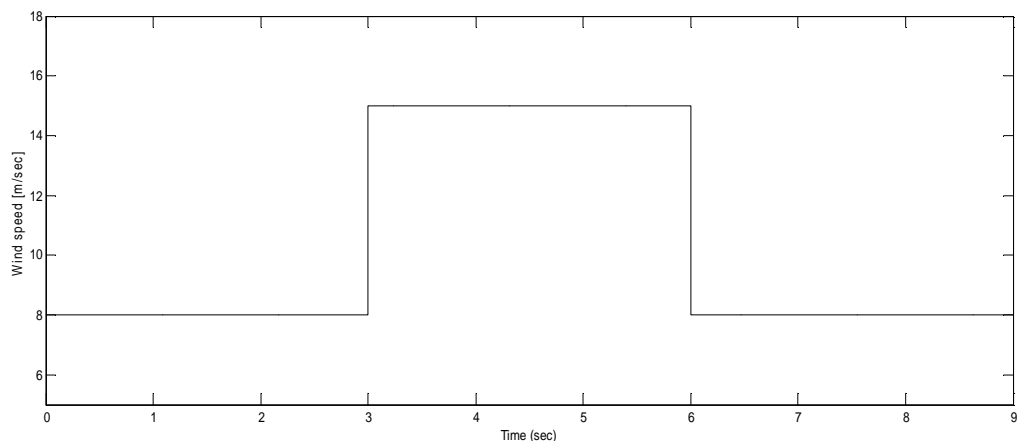
Figure 5: Performance of the proposed DFIG driven by a wind turbine system with wind speed step change with and without the application of FRT scheme during single line to ground fault.

The sequence of operation of the proposed FRT scheme is discussed in Section 4. In response to grid fault, terminal voltage decreases and currents in the stator and rotor circuit increases rapidly, this can be shown in figures 5.h, 5.i and 5.j. As the rotor current exceeds the permissible limit, the gating signals to RSC are blocked. Since the dip in terminal voltage has already surpassed the threshold value, switches S1 and S2 are turned ON and the proposed FRT circuit gets connected to the rotor circuit. Since the FRT circuit is connected, the rotor current subsides below the permissible limit and the gating signals to RSC are restored and generator magnetization is done over the rotor circuit. Now the input mechanical energy of the wind turbine gets stored as electromagnetic energy in the inductor L, instead of being dissipated in the resistor R_{cw} as in the case of an active crowbar. Since the torque balance is achieved between the developed electromagnetic torque of induction machine and the input mechanical torque of the wind turbine as illustrated in figures 5.g and 5.d, so rotor speed are nearly maintained at the pre-fault value as shown in figure 5.b.

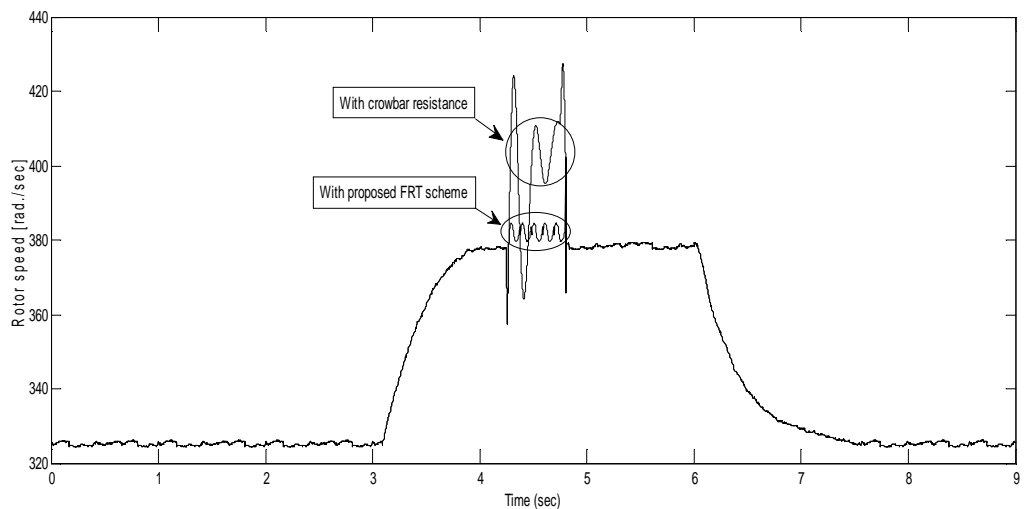
Consequently the reactive power requirement of DFIG on fault clearance shown in figure 5.e is also greatly reduced due to large reduction in rotor speed deviation from its pre-fault value. Hence rapid recovery of terminal voltage of DFIG to nominal voltage, which can be inferred from voltages waveforms, is accomplished with the help of proposed FRT scheme. Also it is clear that the fluctuations in electromagnetic torque and powers of DFIG at the instant of fault clearing are also greatly reduced.

On fault clearing, when the dip in terminal voltage is still below the threshold value, the switches S1 and S2 are turned OFF. Now the diode D gets forward biased and the stored energy in the inductor L is transferred into the dc link capacitor C_{dc} ,

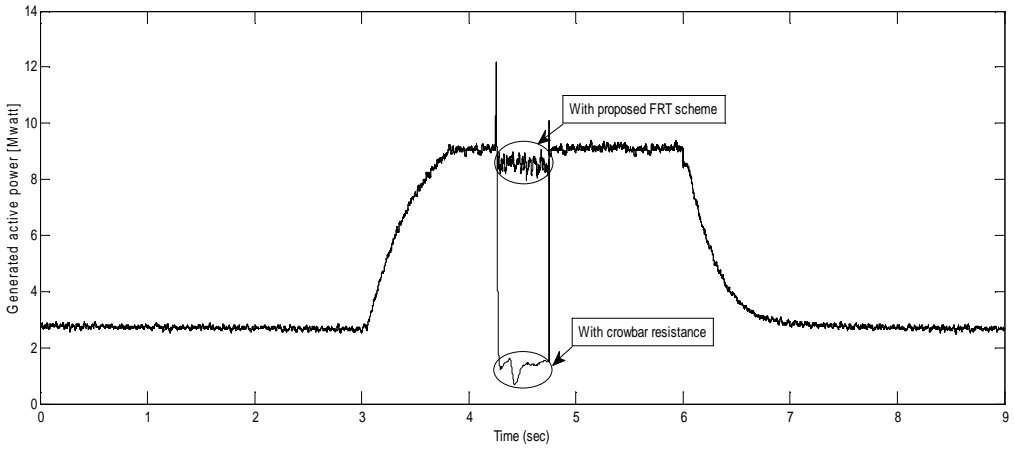
charging it to 1.03 p.u momentarily for a short duration, however it reduces back to its reference value at 4.75 s, this is viewed through figure 5.f. Consequently, the current in GSC needed for charging the dc link capacitor is also reduced and thus the proposed FRT scheme assists GSC and RSC in restoring the normal operation of DFIG as shown in figures 5.i and 5.j, which show the reduction in line and rotor currents after using the proposed scheme. In this scheme, it is observed that the performance of DFIG has improved to a greater extent and comply with the grid code requirements and comply with the grid code requirements.



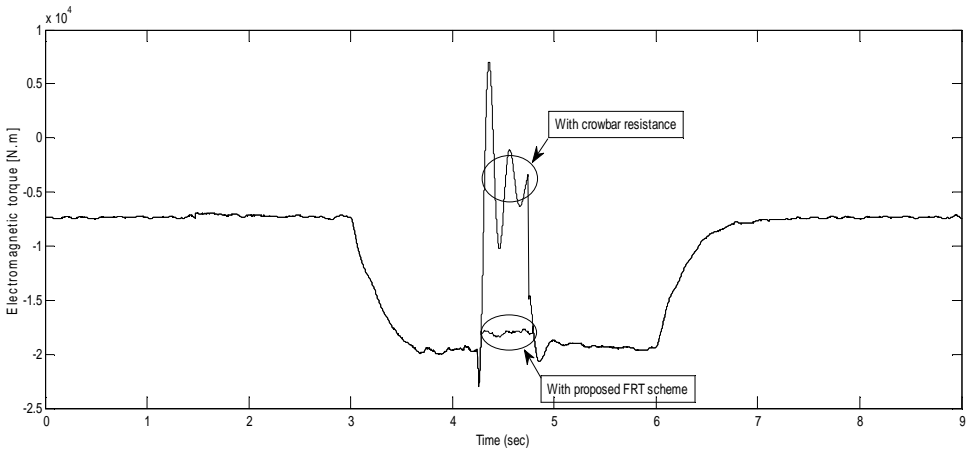
(a) Wind speed variation (m/sec)



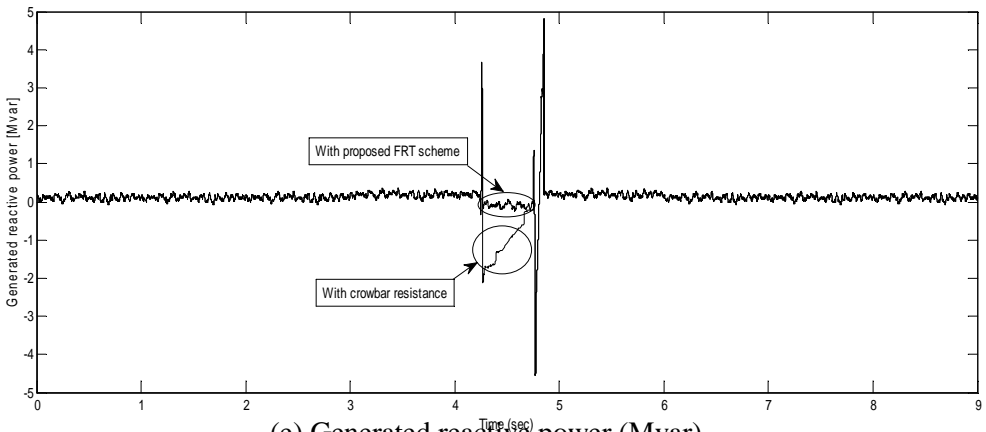
(b) Rotor speed (rad./sec)



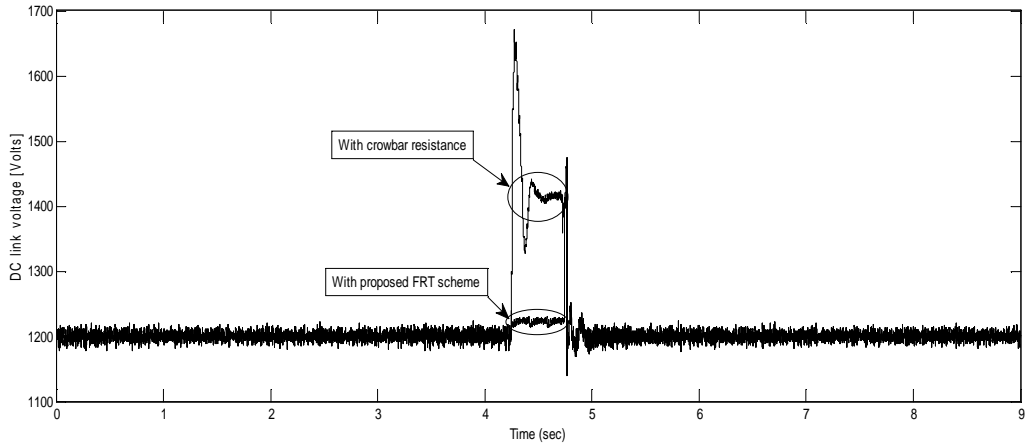
(c) Generated active power (Mwatt)



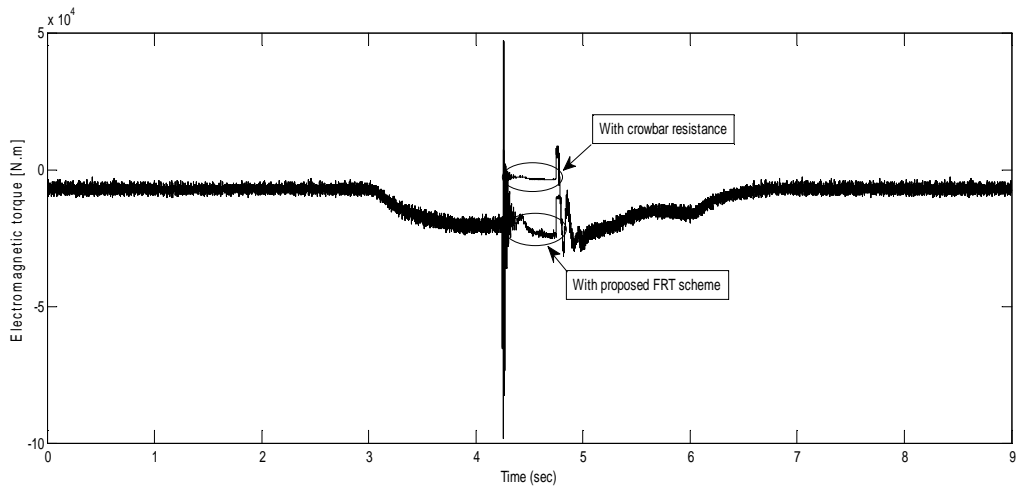
(d) Mechanical torque (N.m)



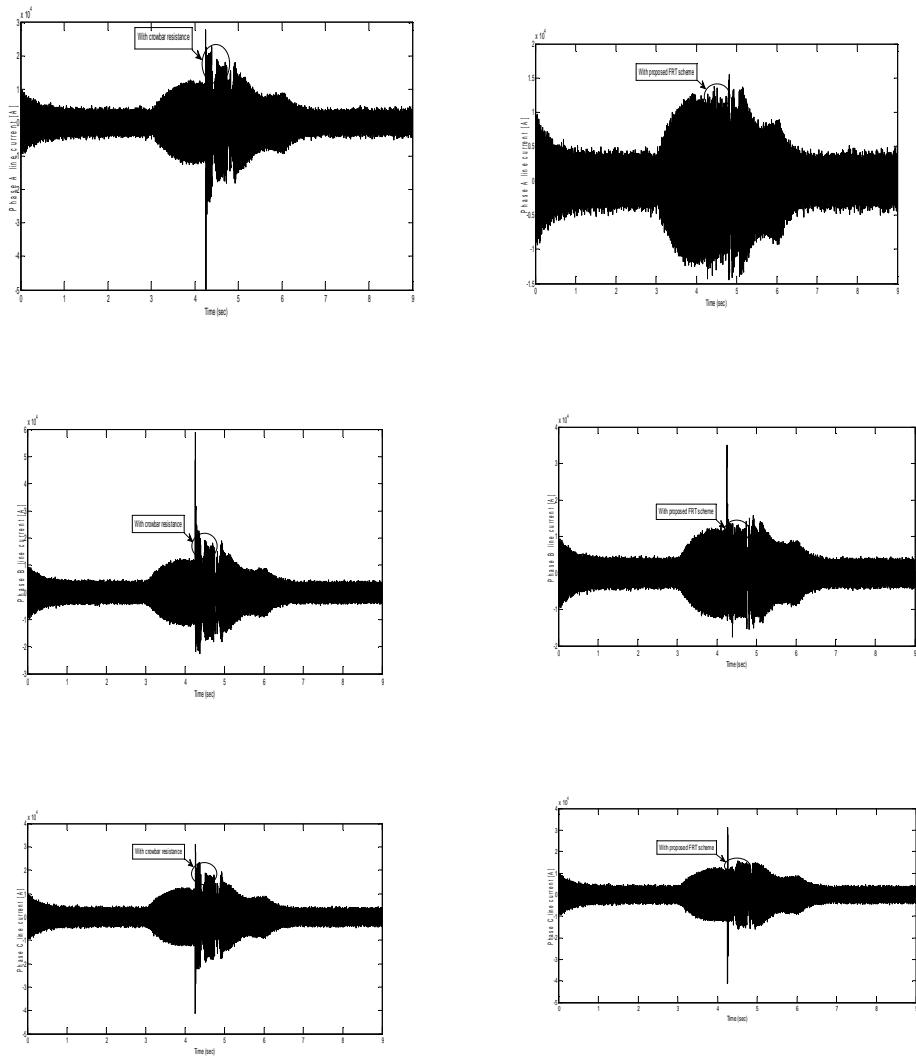
(e) Generated reactive power (Mvar)



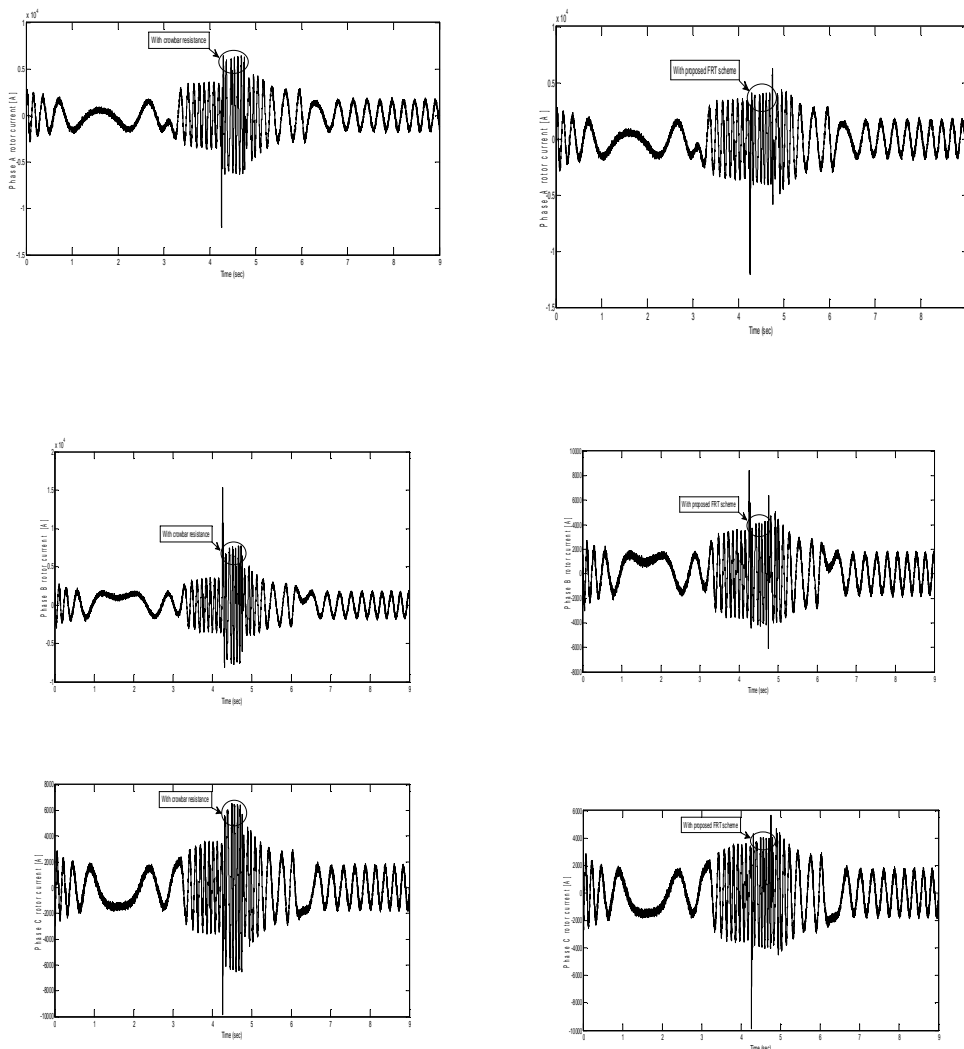
(f) DC link voltage (Volts)



(g) Electromagnetic torque (N.m)



(h) Line currents with and without the application of FRT scheme (A)



(i) Rotor currents with and without the application of FRT scheme (A)

Figure 6: Performance of the proposed DFIG driven by a wind turbine system with wind speed step change with and without the application of FRT scheme during a 3-phase to ground fault.

A Three phase to ground fault was applied across the grid terminals at $t=4.25$ s for 500 ms duration. The performance of the wind generation system under the fault can be observed through figure 6, which illustrates that the generator tends to absorb a large amount of reactive power during fault this can be viewed in figure 6.e, which induces instability in the grid, makes high fluctuation in the active power and line currents which consequently affects the rotor current behavior and the electromagnetic torque of the generator. This can be observed in figure 6.c that shows a severe drop in active power, and figure 5.i which illustrate the increase in rotor currents during fault.

The effect of three phase fault on DFIG's performance can be also investigated through the increase in dc link voltage and severe reduction in both mechanical and electromagnetic torques; this can be shown in figures 6.f, 6.d and 6.g respectively.

After applying the proposed FRT scheme the normal operation of DFIG was restored and the measured values of generated active and reactive power eventually returned to their normal range, this can be shown in figures 6.c and 6.e. Figure 6.f shows the positive effect of proposed scheme on the value of dc link voltage during fault period. The reduction in rotor currents to their normal values can also be viewed in figure 6.i. Both mechanical and electromagnetic torques were obviously affected by applying the scheme, this can be shown through the restoration of their normal values as viewed in figures 6.d and 6.g respectively.

Based on the results of the parameters of DFIG (namely, electromagnetic torque, reactive power and speed) obtained with the proposed FRT scheme, it can be confirmed that the size of inductor chosen in the present study is appropriate and thus the proposed method of computation of initial guess for the size of storage inductor is also validated.

6. CONCLUSION

A novel fault ride-through (FRT) scheme for doubly fed induction generator (DFIG) based wind farm for achieving enhanced performance capabilities in addition to retaining the generator to stay connected to the power system during grid faults is proposed in this paper. The performance of proposed FRT scheme, which uses minimal additional hardware components rated for rotor circuit power rating, is validated for a severe symmetrical grid fault conditions at the terminal of DFIG. Extensive simulation studies employing MATLAB/SIMULINK software is carried out and the performance of the proposed scheme is compared with other existing FRT schemes namely crowbar scheme. In this scheme, the input mechanical energy of the wind turbine during grid fault is stored and utilized at the moment of fault clearance, unlike other existing FRT schemes wherein this is dissipated in the resistors of the crowbar circuit. This results in achieving rotor speed stability, reduced rotor speed deviation and electromagnetic torque fluctuation. Consequently, less reactive power requirement is needed and rapid reestablishment of terminal voltage is attained on fault clearance. Moreover, as the stored energy in the inductor of the proposed scheme is utilized for charging the dc link capacitor on fault clearance, the grid side converter is relieved from charging the dc link capacitor and it can be utilized to its full capacity for rapid restoration of terminal voltage. The simulation results vividly demonstrate the enhanced performance capabilities of proposed FRT scheme employed for DFIG based wind farms.

REFERENCES

- [1] Carrasco JM, Franquelo LG, Bialasiewicz JT, Galvan E, Portillo Guisado RC, Prats MAM, et al. Power-electronic systems for the grid integration of renewable energy sources: a survey. *IEEE Trans Ind Electron* 2006; 53:1002–16.
- [2] Datta Rajib, Ranganathan VT. A method of tracking the peak power points for a variable speed wind energy conversion system. *IEEE Trans Energy Conver*

- 2003; 18:163–8.
- [3] Koutrolis E, Kalaitzakis K. Design of a maximum power tracking system for wind energy conversion applications. *IEEE Trans Ind Electron* 2006; 53:486–94.
 - [4] Srinivasa Rao S, Murthy BK. A new control strategy for tracking peak power in a wind or wave energy system. *Renew Energy* 2009; 34:1560–6.
 - [5] Pena R, Clare JC, Asher GM. Doubly fed induction generator using back-to-back PWM converters and its application to variable-speed wind-energy generation. *IEE Proc Elect Power Appl* 1996; 143:231–41.
 - [6] Grid code regulations for high and extra high voltage Report ENENARHS2006, E.ON, Netz GMBH, Germany 1(April) (2006) 46 (www.eon-netz.com).
 - [7] Piwko Richard, Miller Nicholas, Thomas Girard R, MacDowell Jason, Clark Kara, Murdoch Alexander. Generator fault tolerance and grid codes. *IEEE Power Energy Mag* 2010;8:19–26.
 - [8] Sun T, Chen Z, Blaabjerg F. Voltage recovery of grid connected wind turbines with DFIG after a short circuit fault. 35th Annual IEEE power electronics specialists' conference. Germany: Aschen; 2004. p. 1991–7.
 - [9] Holdsworth L, Wu XG, Ekanayake JB, Jenkins N. Comparison of fixed speed and doubly-fed induction wind turbines during power system disturbances. *IEE Proc-Gener, Transm Distrib* 2003; 150:343–52.
 - [10] Hansen Anca D, Michalke Gabriele. Fault ride through capability of DFIG wind turbines. *Renew Energy* 2007; 32:1594–610.
 - [11] Morren Johen, De Haan Sjoerd WH. Ridethrough of wind turbines with doubly fed induction generator during a voltage dip. *IEEE Trans Energy Conver* 2005; 20:435–41.
 - [12] Seman Slavomir, Niiranen Jouko, Arkkio Antero. Ride-through analysis of doubly fed induction wind power generator under unsymmetrical network disturbance. *IEEE Trans Power Syst* 2006; 21:1782–9.
 - [13] Dittrich Andreas, Stoev Alexander. Comparison of fault ride-through strategies for wind turbines with DFIM generators. In: *Proceeding of European conference on Power electronics and applications*, 11–14 September 2005.
 - [14] Chee-Mun. Ong", *Dynamic Simulation Of Electronic Machinery using Matlab/Simulink*", PRINTICE HALL, (1998).
 - [15] Pete. Vas ", *Vector Control Of AC Machines*", Oxford University, UK.
 - [16] Krause Paul C, Wasynczuk Oleg, Sudhoff Scott D. *Analysis of electric machinery and drive systems*. 2d ed., Piscataway (NJ, USA); IEEE Power Engineering Society, Wiley interscience, John Wiley & Sons Inc 2002.
 - [17] Joshi Nitin, Mohan Ned. A novel scheme to connect wind turbines to the power grid. *IEEE Trans Energy Conver* 2009; 24:504–10.
 - [18] Rahul S . Chokhawala, Jamie Catt, Laszlo Kiraly. A Discussion on IGBT Short-circuit Behavior and Fault Protection Schemes. *IEEE Transactions on industry applications*, Vol. 31, No. 2, Marcw APRIL 1995.
 - [19] Chen Z, Hu Y, Blaabjerg F. Stability improvement of induction generator based wind turbine systems. *IET Renew Power Gener* 2007; 1:81–93.
 - [20] Akhmatov V. Variable speed wind turbines with doubly fed induction generators, Art IV: uninterrupted operation features at grid faults with converter control coordination. *Wind Eng* 2003; 27:519–29.

- [21] Qiao Wei, Venayagamoorthy Ganesh Kumar, Harley Ronald G. Real-time implementation of a statcom on a wind farm equipped with doubly fed induction generators. IEEE Trans Ind Appl 2009; 45:98–107.
- [22] Siegfried Heier, "Grid Integration of Wind Energy Conversion Systems", ISBN 0-471 97143- X, John Wiley & Sons Ltd, (1998).
- [23] Zhou, Y., Bauer, P., Ferreira, J.A., Pierik, J., 2007. Control of DFIG Under Unsymmetrical Voltage Dip. IEEE Power Electronics Specialists Conf., p.933-938. [doi:10.1109/PESC.2007.4342113]
- [24] Xu, L., Wang, Y., 2007. Dynamic modeling and control of DFIG based wind turbines under unbalanced network conditions. IEEE Trans. on Power System, 22(1):314-323. [doi:10.1109/TPWRS.2006.889113]

تعزيز قدرة المولد الحثي المزدوج التغذية المدار بطاقة الرياح والمتصل بالشبكة الكهربائية على تجاوز فترة الخطأ بأداء عالي

تهدف هذه المقالة إلى تعزيز أداء المولد الحثي المزدوج التغذية المدار بطاقة الرياح والمتصل بالشبكة الكهربائية أثناء حدوث أخطاء في الشبكة. وتم تحقيق هذا الهدف من خلال استخدام منظومة تحكم جديدة تتخللها منظومة لتعزيز أداء المولد أثناء فترة الخطأ. المنظومة المقترحة والموجودة بين دائرة العضو الدوار ومكثف جهد الربط ، بالتوازي مع موحد دائرة العضو الدوار (Rotor Side Converter)، تتكون من موحد غير محكوم (Uncontrolled rectifier) ، ومجموعتين من المفاتيح الإلكترونية (IGBTs) ، ودايود وملف. خلال هذه المنظومة يتم تخزين الطاقة الميكانيكية المكتسبة بالتربينة الهوائية أثناء فترة الخطأ، على أن يتم إستخدامها أثناء زوال أثر الخطأ. والك بدلا من ضياع هذه الطاقة كمفاقد حرارية في المقاومات في حالة استخدام دائرة (Crowbar) . وبذلك تم تحقيق الإتزان بين قيم العزم الميكانيكي والكهربى، وبهذا فإن حيود كل من سرعة العضو الدوار والعزم الكهرومغناطيسى عن قيمهم في الحالة العادية أصبح صغير جدا. هذا أيضا أدى إلى عدم الحاجة إلى زيادة القدرة التخيلية أثناء حدوث الخطأ. لوحظ أيضا زيادة قدرة الجهود على استرجاع قيمها الطبيعية بسرعة، أما بالنسبة للطاقة الكهرومغناطيسية المخزنة في الملف فتم تحويلها إلى مكثف جهد الربط والذي يلعب دورا مهما في تثبيت جهد الخط أثناء فترة الخطأ. تم إجراء محاكاة لكل المنظومة بإستخدام الحاسوب (Matlab/Simulink) وذلك لتقدير مدى كفاءة المنظومة المقترحة. وأثبتت النتائج التى تم الحصول عليها أن أداء المولد أثناء فترة الخطأ أصبح جيدا جدا.